Hindawi
Geofluids
Volume 2022, Article ID 6337345, 17 pages
https://doi.org/10.1155/2022/6337345

*Research Article*

# Study on the Strength and Yield Behaviors of Modified Silty Clay

**Yuhang Liu**,[1,2] **Ruiqiang Bai**,[1,2] **and Dongqing Li**[1,2]

[1]*State Key Laboratory of Frozen Soil Engineering, Northwest Institute of Eco-Environment and Resources, Chinese Academy of Sciences, Lanzhou 730000, China*
[2]*University of Chinese Academy of Sciences, Beijing 100049, China*

Correspondence should be addressed to Ruiqiang Bai; rqbai@lzb.ac.cn

Received 8 April 2022; Accepted 27 June 2022; Published 16 July 2022

Academic Editor: Dongdong Ma



To study the strength and yield behaviors of the modified soil, a series of triaxial compression tests were carried out for modified silty clay with different contents of red Pisha sandstone and carbide slag, respectively. The test results showed that the strength variation of the modified soils are obviously nonlinear with the hydrostatic pressure increasing, and the nonlinear strength can be described by a modified critical state function. Then, the friction angle and the cohesive force of the modified soils were obtained according to the nonlinear Mohr-Coulomb equation, and the relationships between the friction angle, the cohesive force, and the hydrostatic pressure were studied. Finally, the yield behavior of the modified soil was investigated based on a generally criterion, and the yield surface of the modified soils locates between the SMP criterion and the Lade-Duncan criterion. This study will help to understand the strength and yield characteristics of modified soils.

## 1. Introduction

With the implementing of "The Belt and Road Initiative," the density of the traffic network will be accumulated, and the traffic volume will increase continuously in cold regions. A growing number of engineerings, such as highways, bridges, and railways, will built in the regions that lack natural and high-quality soils for the foundations. To ensure the constructions service performance and reduce costs, the poor quality filling soils are usually strengthened by different modified methods [1, 2]. Studying the strength and yield behaviors of modified soils will have a great guidance for the constructions of engineering. At present, researches on the strength and yield characteristics of modified soils are less reported, especially on the chemical stabilized soils. Therefore, a study on the strength and yield characteristics of modified soils is needed.

To describe the strength characteristics of geomaterials, many strength criteria or models have been proposed, such as the Mohr-Coulomb criterion (M-C), the Lade-Duncan criterion (L-D), and the Spatially Mobilized Plane criterion (SMP) [3]. In fact, the strength and the yield behaviors of different geomaterials are different, and it is unreasonable to use a specific strength criterion to describe their strength characteristics. To describe the unique properties of geomaterials under various complex stress conditions, these strength criteria were constantly modified and improved [4–6]. Yao et al. [7] proposed a generalized nonlinear strength criterion based on the SMP criterion and the generalized Von Mises criterion. Mortara [8] proposed a widely used nonlinear unified strength criterion (MNLD criterion) based on the SMP criterion and the Lade-Duncan criterion. Liu and Indraratna [9] introduced a material coefficient and proposed a unified strength criterion for frozen soils which achieves the interconversion between the SMP criterion and the Lade-Duncan criterion. Liao et al. and Zhao et al. [10–12] proposed strength criteria of the frozen saline soils by using the generalized nonlinear strength theory, and the criteria can describe the influences of the salt content and the stress states on the strength behaviors. Those researches mainly forced on the strength behaviors of certain structural geomaterials [13]. Besides, comparing with generally structured soils, the strength and yield characteristics of chemical stabilized soils are more complex due to the existence of hydration products [14, 15]. The soils will take place following changes during the improved process:

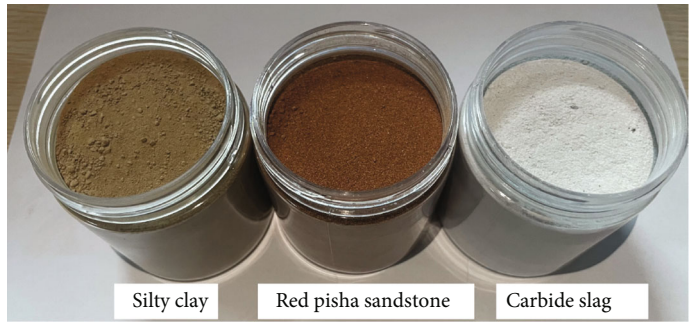


Figure 1: Raw test materials.

(i) the original arrangement of soil particles will be destroyed; (ii) the small particles will aggregate into larger particles, and the particles will be joint by ion exchange, flocculation, and agglomeration; (iii) the hydration products will be formed, which can form a protective film around the soil particles, the pores will be filled, and the permeability will reduce; and (iv) the strength and the stability of soils will increase gradually along with the progress of crystallization. The latter three have greater effect on strength of soils than the first one. The structure and the mineral composition of modified soils will change during the hydration reaction process, so the strength behaviors of modified soils are more complex than that of nature soils. The availability of existing strength criteria on modified soils needs to be studied. Wang et al. [16] researched the yield characteristics of lime modified soil under the conditions of different lime contents. Ren [17] developed a new strength criterion to describe the strength characteristics of nanosilica silty sand. In addition, a strength theory of fly ash stabilized soil is presented based on the Mohr-Coulomb failure criterion and the strength formation mechanism [18]. Based on mentioned above, it can be found that present strength criteria of modified soils are still at the phenomenological stage. The criterion on modified soils needs further improvement. Therefore, it is necessary to verify the availability of existing strength criteria on modified soils and give an effective criterion to describe the strength and yield behaviors of modified soils, which will contribute to the stability and safety of traffic engineering constructions.

In this study, a series of triaxial compression tests for modified soils (red Pisha sandstone and carbide slag stabilized soils) were carried out. The nonlinear strength behaviors of the modified soils were studied, and the behaviors can be described by a nonlinear critical state function. Also, the friction angle and the cohesive force of the modified soils were studied. Meanwhile, the availability of a generalized nonlinear yield criterion on modified soils was verified. This study will contribute to the understanding of the strength and yield characteristics of modified soil.

## 2. Test Procedure

*2.1. Test Material.* The tested silty clay was obtained from a highway construction field in Lanzhou, China. And the rad

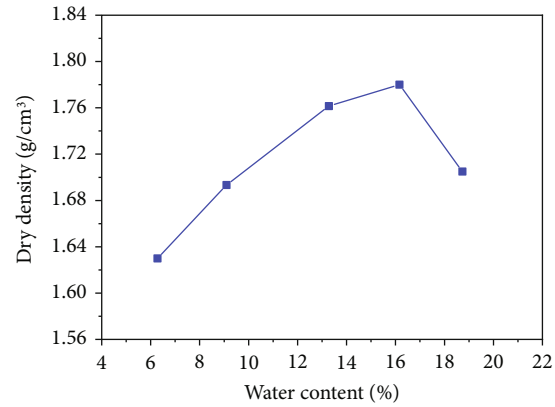


Figure 2: The relationship curve of water content and dry density of silty clay.

Pisha sandstone (RPS) and the carbide slag (CS) were collected from Yanglin, China. The raw test materials are shown in Figure 1. The relationship curve of water content and dry density of the silty clay is showed in Figure 2. The grain size distribution of the raw test materials are shown in Figure 3. The basic physical parameters of the test materials are listed in Table 1.

*2.2. Sample Preparation and Test Procedures.* The mix proportions of the admixture are listed in Table 2. The soil and admixtures were filtered with 2 mm sieve after air-drying and crushing. Next, the admixtures and the silty clay were mixed, and the required water was added. According to Figure 2, the initial water content and dry density of all samples were kept as constant values of 16% and 1.65 g/cm$^3$, respectively. The samples were prepared as cylinders with 39.1 mm in diameter and 80.0 mm in height. The samples were wrapped and insulated in plastic bags to prevent evaporation after removing the moulds. The samples were subsequently cured at 20°C ± 2°C and relative humidity of 95% ± 3% for 7 days before testing.

A series of triaxial compression tests were conducted by a GDS unsaturated soil triaxial system as shown in Figure 4(a) [19]. The sample was loaded at a constant axial displacement rate of 0.4 mm/min in unconsolidated and undrained test methods. The confining pressure was controlled as 100 kPa, 200 kPa, and 400 kPa, respectively. The load and deformation data were recorded and stored by

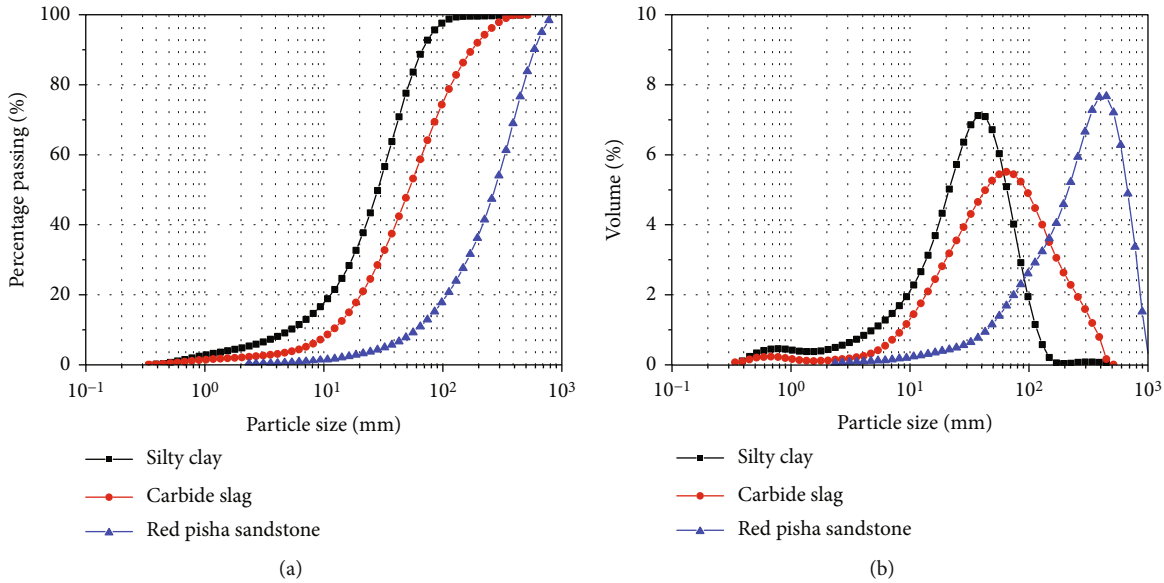


Figure 3: Grain size distributions of the test materials: (a) percentage passing; (b) volume distributions [19].

Table 1: Basic physical parameters of raw test materials [19].

| Property | Silty clay | Red Pisha sandstone | Carbide slag |
|---|---|---|---|
| Liquid limit, $w_L$ (%) | 28.35 | 29.03 | 41.83 |
| Plastic limit, $w_P$ (%) | 13.04 | 19.60 | 32.01 |
| Plasticity index, $I_p$ | 15.31 | 9.43 | 9.82 |
| Maximum dry density, $\rho_{d,max}$ (g/cm$^3$) | 1.78 | 1.96 | 1.90 |
| Optimum moisture content, $w_{opt}$ (%) | 16.16 | 12.00 | 13.40 |
| Specific surface area (m$^2$/g) | 11.46 | 3.39 | 10.30 |
| Particle size distribution (%) | | | |
| Clay (<5 $\mu$m) | 9.61 | 0.00 | 3.83 |
| Silt (5 $\mu$m to75 $\mu$m) | 83.31 | 6.64 | 60.67 |
| Sand (>75 $\mu$m) | 7.08 | 93.36 | 35.50 |

Table 2: Mix proportion of the test materials [19].

| Type | Solid powder mix proportions (wt.%) | | |
|---|---|---|---|
| | Silty clay | Red Pisha sandstone | Carbide slag |
| A | 100 | 0 | 0 |
| B1 | 90 | 10 | 0 |
| B2 | 85 | 15 | 0 |
| B3 | 80 | 20 | 0 |
| C1 | 90 | 0 | 10 |
| C2 | 85 | 0 | 15 |
| C3 | 80 | 0 | 20 |
| D1 | 85 | 10 | 5 |
| D2 | 80 | 10 | 10 |
| E1 | 80 | 15 | 5 |
| E2 | 75 | 15 | 10 |
| E3 | 70 | 15 | 15 |

the data acquisition system during the tests. Once the axial deformation reachs 15%, the test is stopped [20], and the samples after test are shown in Figure 4(b).

## 3. Test Results and Analyses

Since the curves behaviors were approximately similar within the tested confining pressure range, the deviatoric stress-train curves of the samples E1-E3 as a case study. From Figure 5, it can be found that the soil exhibits a strain-hardening behavior under the confining pressures of 100 kPa and 200 kPa, and it exhibits a strain softening characteristic under the confining pressure of 400 kPa. This indicates that the strain-hardening behavior of the modified soils gradually changes to a strain-softening behavior with the increase of confining pressure.

According to the China Geotechnical Test Standards [20], the stress at the peak deviatoric stress (softening behavior) or the stress at the 15% axial strain (hardening or plastic

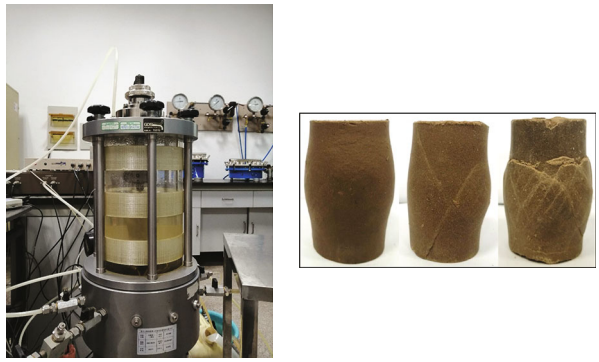

(a) (b)

Figure 4: Testing system and soil sample: (a) the GDS triaxial test apparatus; (b) the samples after test [19].

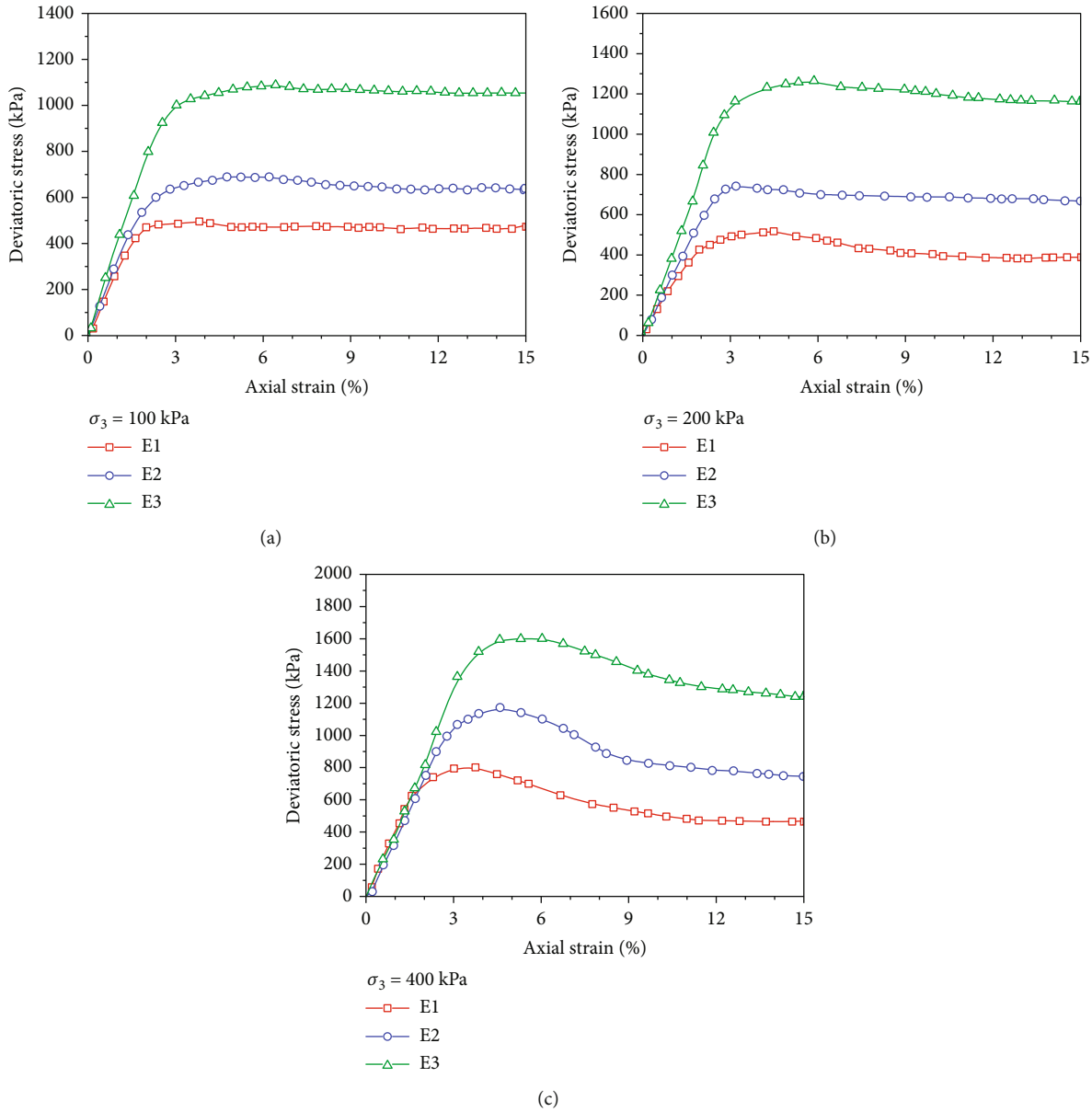


Figure 5: Deviatoric stress-strain curves of the samples E1-E3 under different confining pressures: (a) $\sigma_3$ = 100 kPa; (b) $\sigma_3$ = 200 kPa; and (c) $\sigma_3$ = 400 kPa [19].

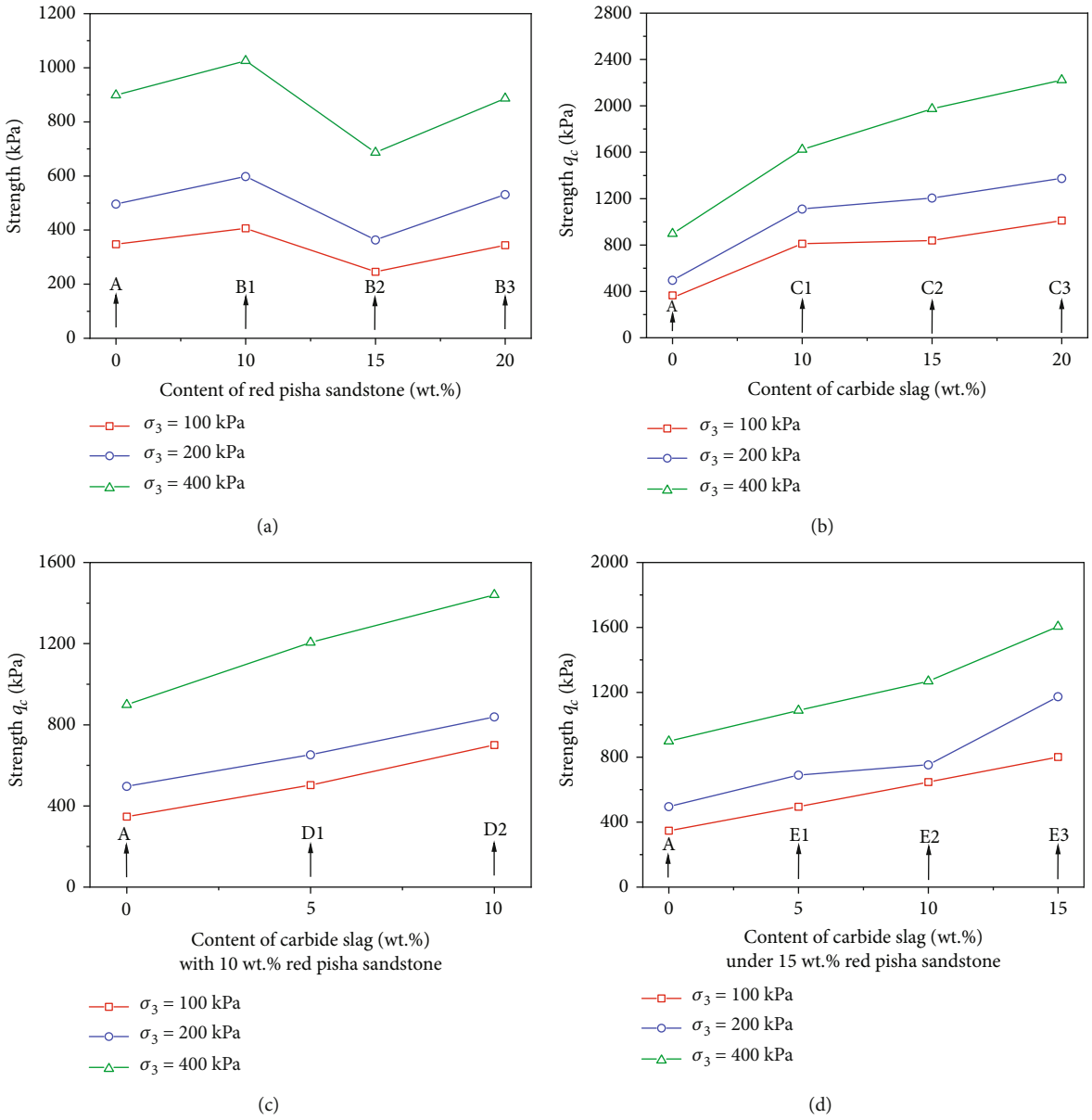


Figure 6: Strength of the modified soils under different confining pressures: (a) the red Pisha sandstone modified soils; (b) the carbide slag modified soils; (c) the red Pisha sandstone and carbide slag modified soil; and (d) the red Pisha sandstone and carbide slag modified soil.

behavior) of the stress-strain curve can be defined as the triaxial compressive strength. Thus, the strengths of the modified soils with admixtures contents under different confining pressures are shown in Figure 6. It can be found that the strength increases with the increase of confining pressure under the condition of constant admixture content. For red Pisha sandstone stabilized soils (samples B1-B3), by increasing red Pisha sandstone content under constant confining pressure condition, the strengths do not obviously change compared with pure silty clay (sample A), as shown in Figure 6(a). When 15 wt.% red Pisha sandstone is added to the silty clay, the strength is even smaller than the pure silty clay. For the carbide slag stabilized soils (samples C1-C3) which only contains carbide slag, the strength increases obviously with the increase of carbide slag content as shown in Figure 6(b). For the red Pisha sandstone and carbide slag stabilized soils (samples D1-E3), in which carbide slag and red Pisha sandstone are mixed into the soil, the strength of sample E3 is maximum under different confining pressures, as shown in Figures 6(c) and 6(d). On the whole, under certain add amount of red Pisha sandstone, the strength of the sample positively correlates with the carbide slag content. However, the strength growth rate is obviously different with the increase of admixture content. In other words, a nonlinear relationship is found between the strength and admixture content.

These nonlinear phenomena are analyzed and discussed from two aspects as follows:

The first is the particle size distribution. Some studies have shown that soil is an assembly of soil particles that

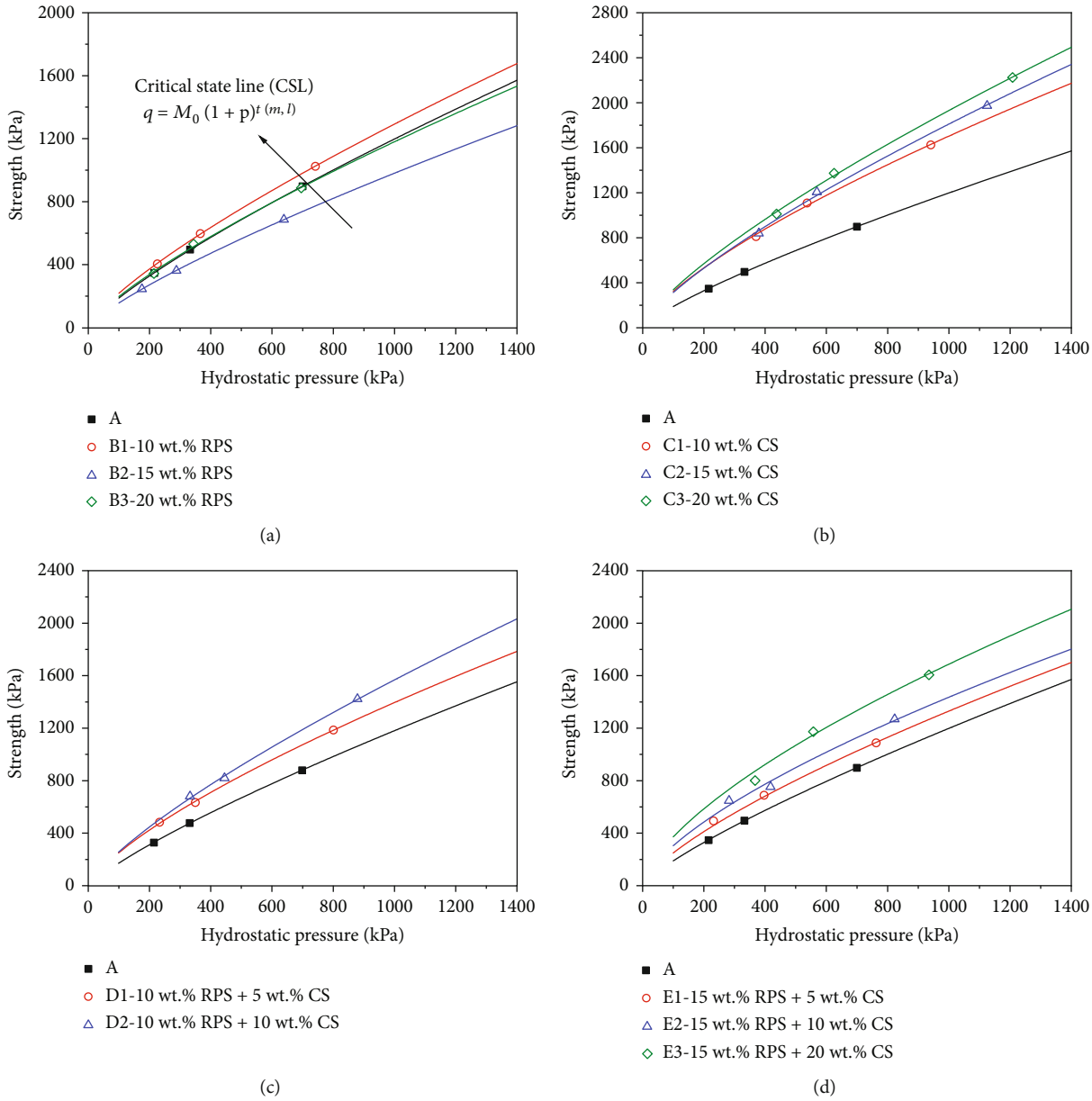


Figure 7: Critical state lines of modified soils: (a) the red Pisha sandstone modified soils; (b) the carbide slag modified soils; (c) the red Pisha sandstone and carbide slag modified soils; and (d) the red Pisha sandstone and carbide slag modified soils.

are more prone to relative slip damage than soil particles themselves. When a certain content of coarse particles are added to the soil, the strength will be improved. At this point, coarse particles play the role of soil skeleton. When the content of the coarse particles exceeds a certain value, the adhesion between continuous particles will decrease gradually. The specimen has a loose structure due to more pores, so the strength of the soil will reduce [4, 21–23]. In addition, it is also found that the void of the soil can be reduced, which will become compact with the increase of fine particles. Assuming that fine particles and coarse particles are from the same origin (same mineralogical components, same particle shape, and so on), there is an inverse correlation between the strength and the proportion of large pores [24, 25]. Hence, for the red Pisha sandstone modified soil, it can be considered that the red Pisha sandstone increases the content of coarse particles in the soil combined with Figure 1. The soil with red Pisha sandstone content of 15 wt.% is the inflection point of strengths in Figure 6(a). After the point, the adhesion between continuous soil particles and strength will reduce. For the carbide slag modified soils, the carbide slag mainly increases the contents of silt particles and clay particles. The strength increases with the increase of carbide slag content. For the red Pisha sandstone and carbide slag modified soils when the content of red Pisha sandstone is constant, the strength increases with the increase of fine particle content (carbide slag content), as shown in Figures 6(c) and 6(d).

The second is the hydration reaction process. Studies have shown that natural red Pisha sandstone can partly

dissolve in alkali solutions, in which the active $SiO_2$ and $Al_2O_3$ in red Pisha sandstone form geopolymer gels will dissolve. But the dissolution rates of the active $SiO_2$ and $Al_2O_3$ are insufficient to produce a binder. The additions of carbide slag, blast furnace slag, lime, or fly ash result in a large number of geopolymers and hydration products form in red Pisha sandstone; thus, the strength will increase [21, 26–28]. In addition, the carbide slag has a finer particle size and greater specific surface area than the above alkali materials. It can lead to soil particle flocculation and agglomeration at early stage, and pozzolanic reactions are more adequate during the entire curing process [29]. A large number of hydration products and gels form, which are the major contributor for the modified soil strength, and the strength increase with the increasing of reaction products [29–31].

Based on this perspective, there is no reaction or very little reaction in the red Pisha sandstone modified soils which will increase the binders. For carbide slag modified soils, the soil particle flocculation and agglomeration at the early stage and pozzolanic reactions during the entire curing process result in the formation of gels. The denser soil structure and the great strength can be obtained than pure silty clay. For red Pisha sandstone and carbide slag modified soils, the clay minerals (e.g., kaolin, feldspar, and cronstedtite) have poor water erosion resistance in pat of the red Pisha sandstone, which was consumed to yield Si and Al for the production of Si-Al gels under the action of an alkali solution [26]. When used as the mineral additive, the carbide slag greatly promotes the polymerization reaction of the Si-Al gels by providing active Si and Al to synthesize more Si-Al gels, C-S-H gels (calcium silicate hydrates), and C-A-S-H gels (calcium aluminosilicate hydrates). They are produced of the hydration reaction of carbide slag. These Si-Al gels improve the properties of the modified soil due to the good water erosion resistance and high strength. Another part of the red Pisha sandstone acts as the skeleton of the soil. Wide pore channels exist in the soils, and this structure is conducive to the hydration reaction. The more content of carbide slag in the soil, the more obvious chemical reaction; the more gels are, the more obvious effect of improving its strength is.

Hence, the nonlinear relationship between the strength and admixture content may be caused by the combination of the particle size distribution and the hydration reaction.

## 4. Strength and Yield Behaviors of the Modified Silty Clay

### 4.1. The Influence of Admixtures Content on the Strength Behavior

*4.1.1. The Influence of Admixtures Content on the Critical State Lines.* To describe the strength characteristics of soils, Roscoe and Burland [32] proposed the concept of the critical state. The critical state curve can be expressed by a linear relationship in the $p-q$ plane:

$$\begin{cases} q = M_0 p & (c = 0) \\ q = M_0 p + q_c & (c \neq 0), \end{cases} \tag{1}$$

Table 3: Parameters of critical strength with different admixtures contents.

| Type | $M_0$ | $t(m,l)$ | $R^2$ |
|---|---|---|---|
| A | 4.597 | 0.805 | 0.999 |
| B1 | 6.155 | 0.774 | 0.998 |
| B2 | 5.476 | 0.778 | 0.993 |
| B3 | 3.960 | 0.798 | 0.999 |
| C1 | 11.412 | 0.775 | 0.994 |
| C2 | 9.183 | 0.765 | 0.995 |
| C3 | 10.139 | 0.760 | 0.997 |
| D1 | 9.427 | 0.765 | 0.998 |
| D2 | 8.034 | 0.725 | 0.996 |
| E1 | 8.566 | 0.730 | 0.997 |
| E2 | 13.429 | 0.716 | 0.970 |
| E3 | 17.744 | 0.704 | 0.994 |

where $q$ is the strength, $p$ is the hydrostatic pressure, $p = (\sigma_1 + \sigma_2 + \sigma_3)/3$, $c$ is the cohesive force, $M_0$ is the initial critical stress ratio, and $q_c$ is the intercept of the critical state curve.

From Figure 6, it can be found that the critical state lines of the modified soils are nonlinear. Therefore, the critical strength functions for the soils can be modified as

$$q = M_0(1+p)^{t(m,l)}, \tag{2}$$

where $t(m,l)$ is the material parameter related to the admixture content and the admixture type, which reflects the change of strength with the admixture, and $m$ and $l$ are the contents of the red Pisha sandstone and the carbide slag, respectively.

The critical state function in the $p-q$ plane can be expressed by

$$f(p,q) = M_0(1+p)^{t(m,l)} - q = 0. \tag{3}$$

The static critical lines of the modified soils with different admixture contents are shown in Figure 7 (the points are the measured results and the curves are the critical state lines). The parameters are given in Table 3. And the material parameters ($m$ and $l$) related to admixture contents can be expressed as

$$t(m,0) = 3.40336m^3 + 1.7345m^2 - 0.5197m + 0.8052, R^2 = 0.995, \tag{4}$$

$$t(0,l) = 19.337l^3 - 4.7515l^2 - 0.0252l + 0.8052, R^2 = 0.996, \tag{5}$$

$$t(0.1,l) = 23.984l^2 - 2.8016l + 0.8053, R^2 = 0.997, \tag{6}$$

$$t(0.15,l) = -78.491l^3 + 23.978l^2 - 2.5029l + 0.8053, R^2 = 0.995. \tag{7}$$

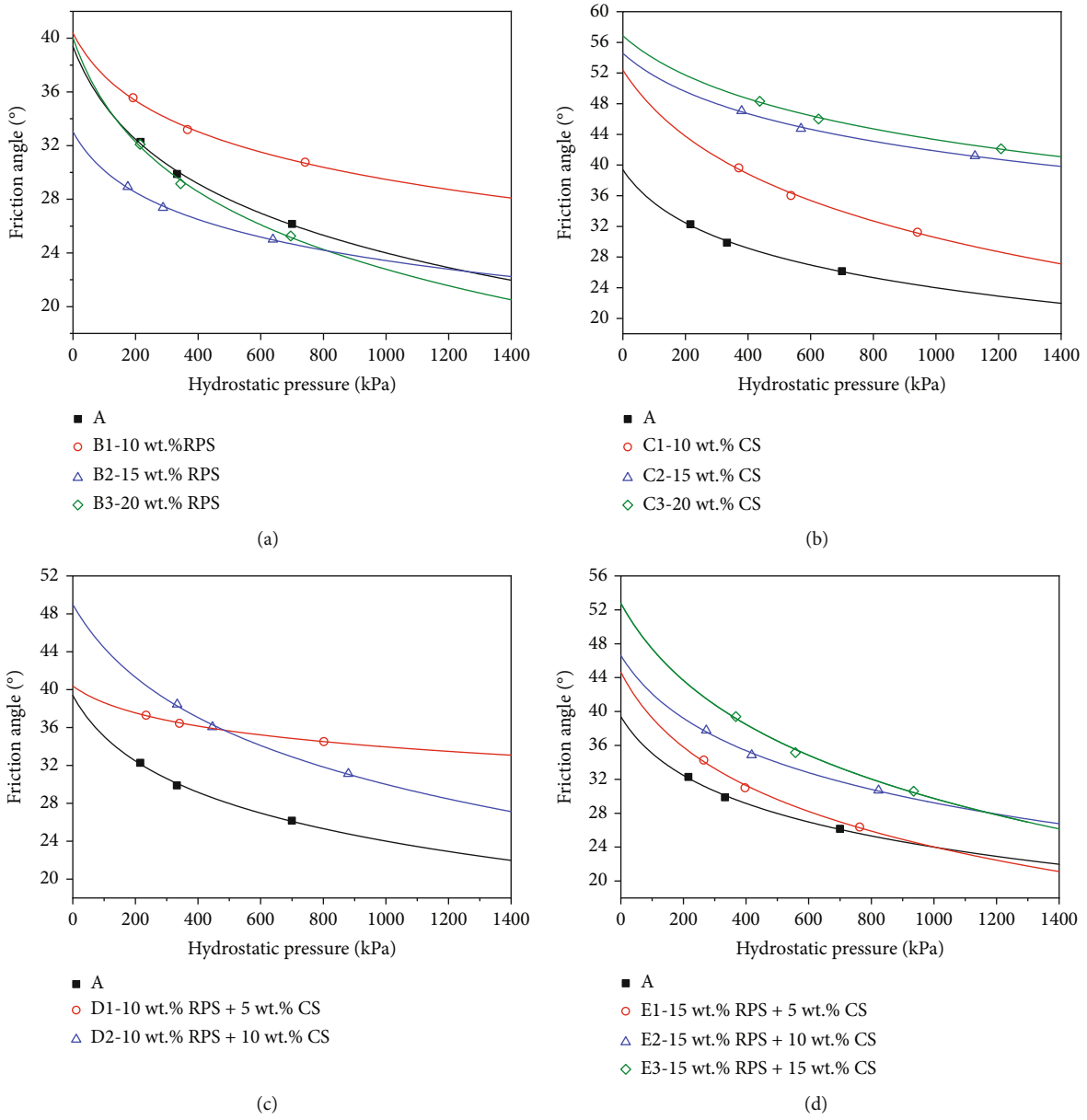


Figure 8: Relationships between the hydrostatic pressure and the friction angle for the modified soils: (a) the red Pisha sandstone modified soils; (b) the carbide slag modified soils; and (c, d) the red Pisha sandstone and carbide slag modified soils.

From the Figure 7, the following can be observed:

(1) The static critical lines (CSLs) of the modified soils with different admixture contents are nonlinear, and the slope of the CSLs is positive under all hydrostatic pressure

(2) The CSL slopes of the different modified soils are different under the same confining pressure. Assume that the slope of pure silty clay is $t_0$ and $t_{15wt.\%} < t_{20wt.\%} < t_{10wt.\%} < t_0$ for red Pisha sandstone stabilized soils; but the $t_{10wt.\%} < t_{15wt.\%} < t_{20wt.\%} < t_0$ for carbide slag stabilized soils

Some studies suggest that the admixture modification of the soil microstructure may lead to deformations at the macroscopic scale, and these deformations significantly influence the mechanical behavior of the soil [4]. After being improved, the arrangement of soil particles and the inter particle cementation also have a significant influence on the mechanical properties of soil. Thus, the critical state line (CSL) changes with the changes of fine particles content and hydration products in the soil. In Figure 7(a), the nonlinear degree of the curves increases with the increase of red Pisha sandstone content. It can be found that the critical state line of sample B3 almost coincides with that of pure silty clay. With the increase of the red Pisha sandstone content, the

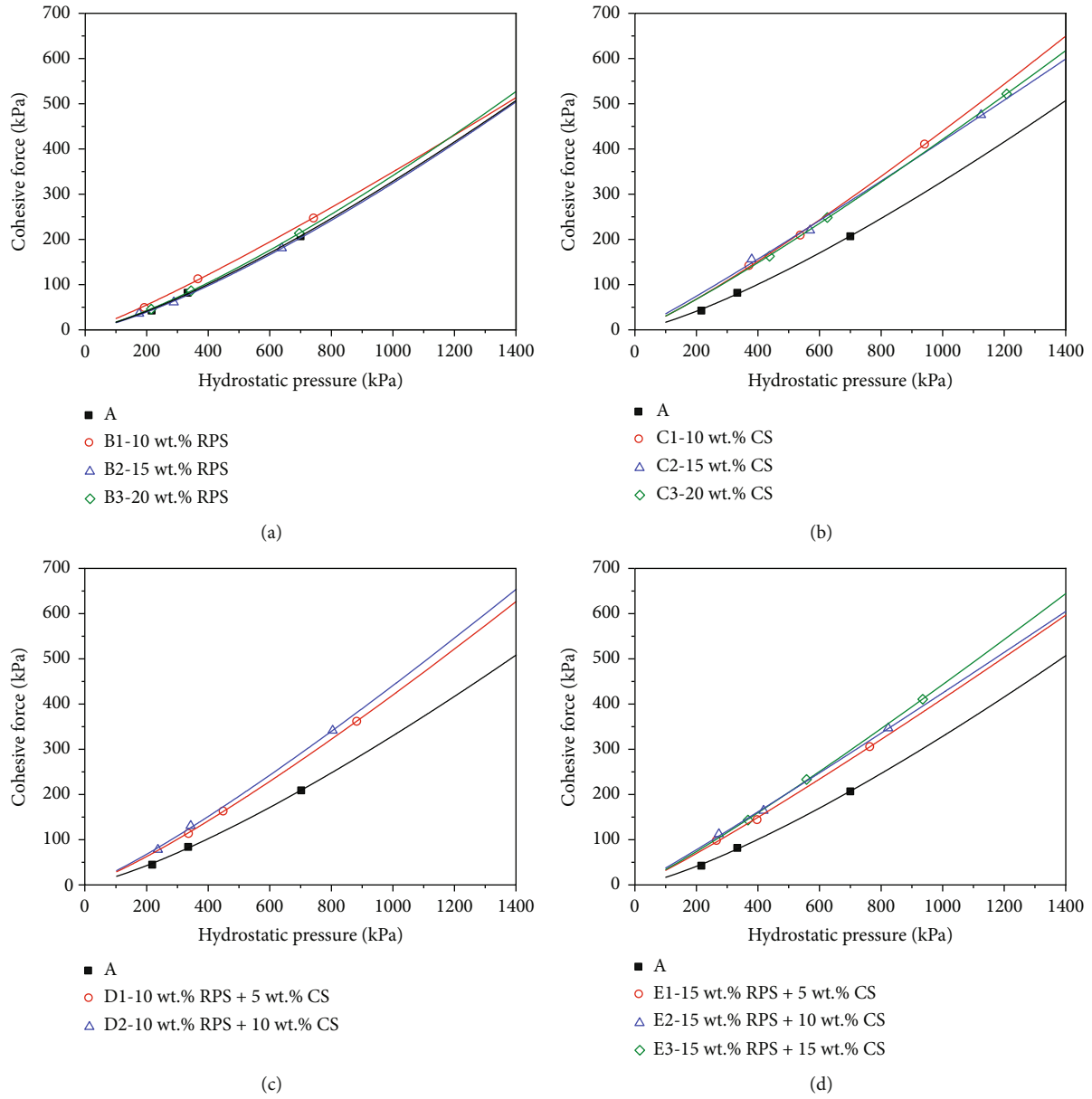


Figure 9: Relationships between the hydrostatic pressure and the cohesive force for the modified soils: (a) the red Pisha sandstone modified soils; (b) the carbide slag modified soils; and (c, d) the red Pisha sandstone and carbide slag modified soils.

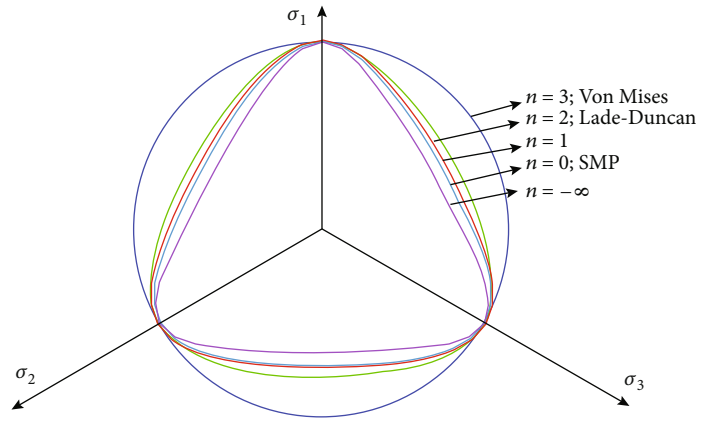


Figure 10: Influence of parameter $n$ on the yield curve in deviatoric plane.

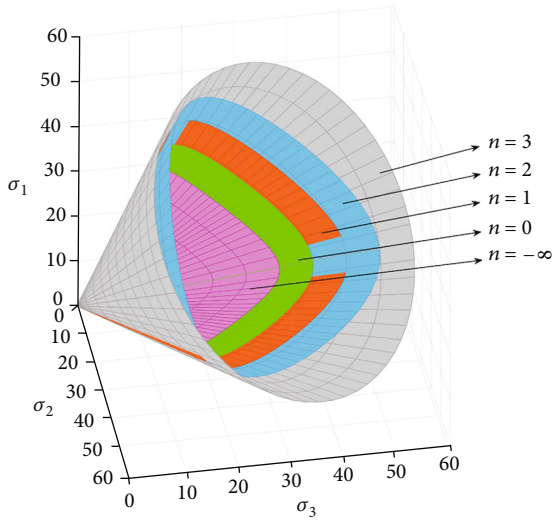


Figure 11: Yield surfaces under different $n$ values.

parameter $M_0$ decreases gradually, and the parameter $t$ has little change. From Figures 7(b)–7(d), it can be found that the nonlinear degree of the curve becomes more obvious with the increase of carbide slag content under a certain red Pisha sandstone content (0 wt.%, 10 wt.%, and 15 wt.%). Comparing the curves of samples D1 with E1, and D2 with E3, we can find that the nonlinear degree of the curve increases with the increasing of red Pisha sandstone content under a certain admixtures content of carbide slag. We can be sure that the influence of red Pisha sandstone on strength nonlinear degree is greater than that of carbide slag.

*4.1.2. The Influences of Admixtures Content on the Friction Angle and the Cohesive Force.* In the $\sigma - \tau$ space, the criterion of Mohr-Coulomb can be expressed as

$$F(\sigma_1, \sigma_3) = \left(\sigma - \frac{\sigma_1 + \sigma_3}{2}\right)^2 + \tau^2 - \left(\frac{\sigma_1 - \sigma_3}{2}\right)^2 = 0. \tag{8}$$

In the $p - q$ space, the criterion can be expressed as follows:

$$F(p, q) = \left(\sigma - p - \frac{q}{6}\right)^2 + \tau^2 - \frac{q^2}{4} = 0. \tag{9}$$

According to the envelope theory, the following equation can be obtained:

$$\frac{\partial F}{\partial p}\frac{\partial f}{\partial q} - \frac{\partial F}{\partial q}\frac{\partial f}{\partial p} = 0. \tag{10}$$

Substituting Equations (3) and (9) into Equation (10), for the nonlinear strength criterion of modified soil, the normal stress $\sigma$ related to $p$ and $q$ can be obtained by

$$\sigma = \frac{(1/3p - 4/9q)\left[M_0 \cdot t(m,l) \cdot (1+p)^{t(m,l)-1}\right] + 2p + 1/3q}{2 + 1/3\left[M_0 \cdot t(m,l) \cdot (1+p)^{t(m,l)-1}\right]}, \tag{11}$$

$$\tau = \sqrt{\frac{q^2}{4} - \left\{\frac{((1/3)p - (4/9)q)\left[M_0 \times t(m,l) \times (1+p)^{t(m,l)-1}\right] + 2p + (1/3)q}{2 + (1/3)\left[M_0 \times t(m,l) \times (1+p)^{t(m,l)-1}\right]} - p - \frac{1}{6}q\right\}^2}. \tag{12}$$

In the $\sigma - \tau$ space, the friction angle of the modified soil can be calculated by

$$\tan\varphi = \frac{d\tau}{d\sigma} = -\frac{\partial f/\partial\sigma}{\partial f/\partial t} = -\frac{\sigma - p - (1/6)q}{\tau}, \tag{13}$$

$$\varphi = \arctan\left(-\frac{\sigma - p - (1/6)q}{\tau}\right). \tag{14}$$

Substituting Equations (11) and (12) into Equation (14), the friction angle $\varphi$ and the cohesive force $c$ can be obtained as follows:

$$\varphi = \arctan\left(-\frac{\left(((1/3)p - (4/9)q)\left[M_0 \times t(m,l) \times (1+p)^{t(m,l)-1}\right] + 2p + (1/3)q\right)/\left(2 + (1/3)\left[M_0 \times t(m,l) \times (1+p)^{t(m,l)-1}\right]\right) - p - (1/6)q}{\sqrt{(q^2/4) - \left\{\left(((1/3)p - (4/9)q)\left[M_0 \times t(m,l) \times (1+p)^{t(m,l)-1}\right] + 2p + (1/3)q\right)/\left(2 + (1/3)\left[M_0 \times t(m,l) \times (1+p)^{t(m,l)-1}\right]\right) - p - (1/6)q\right\}^2}}\right), \tag{15}$$

$$c = \sqrt{\frac{q^2}{4} - \left\{\frac{((1/3)p - (4/9)q)\left[M_0 \times t(m,l) \times (1+p)^{t(m,l)-1}\right] + 2p + (1/3)q}{2 + (1/3)\left[M_0 \times t(m,l) \times (1+p)^{t(m,l)-1}\right]} - p - (1/6)q\right\}^2} - \frac{((1/3)p - (4/9)q)\left[M_0 \times t(m,l) \times (1+p)^{t(m,l)-1}\right] + 2p + (1/3)q}{2 + (1/3)\left[M_0 \times t(m,l) \times (1+p)^{t(m,l)}\right]} \tan\varphi, \tag{16}$$

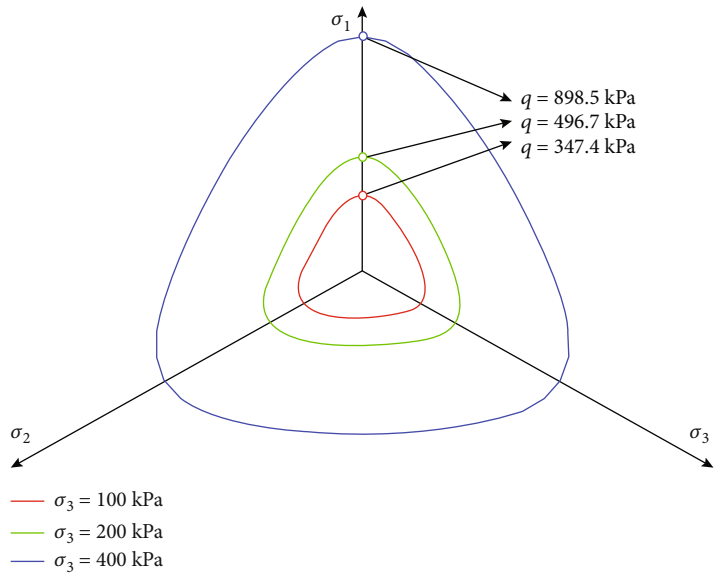


Figure 12: Yield curves of the silty clay under different confining pressures.

Combining with Table 3, the relationship between hydrostatic pressure and the friction angle of the modified soils with different admixture contents can be obtained by Equation (15), as shown in Figure 8. It can be found that the friction angles of all samples decrease with the increase of hydrostatic pressure. For red Pisha sandstone modified soils, the friction angle reaches the minimum and maximum values when red Pisha sandstone contents are 15 wt.% and 10 wt.%, respectively (Figure 8(a)). The friction angle of sample B3 (20 wt.% red Pisha sandstone) is the same as that of pure silty clay (sample A). For the carbide slag modified soils, the friction angles increase with the increase of admixture contents (Figure 8(b)). For the red Pisha sandstone and carbide slag modified soils, the friction angles are positively correlated with the carbide slag contents under a certain admixtures content of red Pisha sandstone (Figures 8(c) and 8(d)). On the whole, the influence of hydrostatic pressure on friction angle of sample D2 is little, and only the friction angle of sample B2 is less than that of pure silty clay.

The relationships between the hydrostatic pressure and the cohesive force of the modified soils with different admixture contents are shown in Figure 9. As can be seen, there is a positive correlations between the cohesive force and the hydrostatic pressure. In Figure 9(a), the content of red Pisha sandstone has little influence on the curves. The cohesive force of sample B3 is slightly higher than that of other soil samples. The cohesive forces of the carbide slag modified soils are significantly higher than that of silty clay with the increase of hydrostatic pressure (Figure 9(b)). For the red Pisha sandstone and carbide slag modified soils, the cohesive force increases with the increase of hydrostatic pressure and carbide slag content (Figures 9(c) and 9(d)).

### 4.2. Yield Behaviors of the Modified Silty Clay

*4.2.1. Yield Criterion of the Modified Silty Clay.* Numerous theoretical researches have shown that the yield curves of different geomaterials in the deviatoric plane are constantly changing, and it is impossible to use a specific criterion to describe their yield characteristics. Hence, in order to apply to various complex stress conditions and unique properties of geomaterials, some criteria are constantly proposed [2, 6–11, 33]. Chen [2] proposed a criterion based on the generalized Von Mises criterion, the Lade-Duncan criterion, and the SMP criterion, which can be expressed as

$$\frac{I_1 I_2^{1-n/2}}{I_3^{1-n/3}} = k_i, \tag{17}$$

where $I_1$, $I_2$, and $I_3$ are the first stress invariant, the second stress invariant, and the third stress invariant, respectively; and $n$ and $k_i$ are the material parameters.

The value of the parameter $n$ reflects the shape change of the yield curve: (i) when $n$ is equal to 3, the yield curve degenerates to generalized Von Mises criterion; (ii) when $n$ is equal to 2, the yield curve degenerates to the Lade-Duncan criterion; (iii) when $n$ is equal to 0, the yield curve degenerates to the SMP criterion; (iv) when $n$ is in the range of 0 to 3, the criterion between the generalized Von Mises criterion and the SMP criterion, which applies to soil, rock, concrete, and other materials; and (v) when $n$ is less than 0, the yield curve in the inside of the SMP criterion, which is suitable for brittle materials. The generalized Von Mises criterion, the Lade-Duncan criterion, and the SMP criterion are special cases of this generalized criterion. For $k_i$ is a constant, the curves in the deviatoric plane for different parameters $n$ (from -∞ to 3) are shown in Figure 10. In this case,

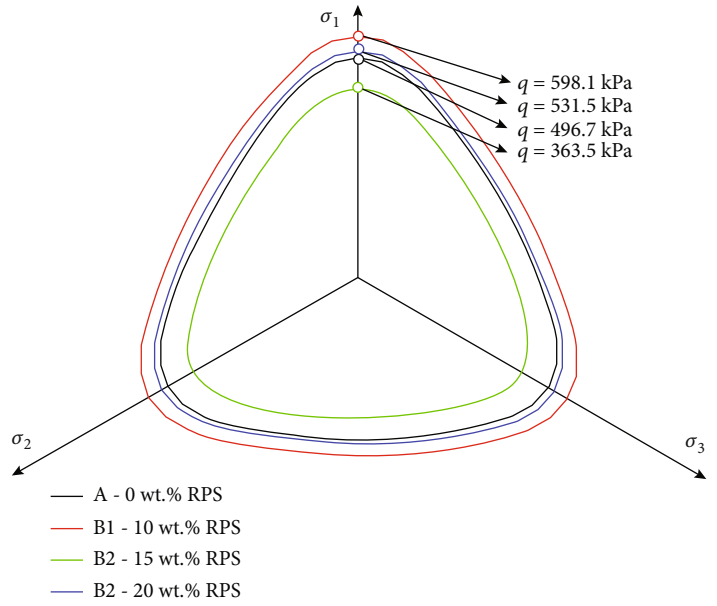


(a)

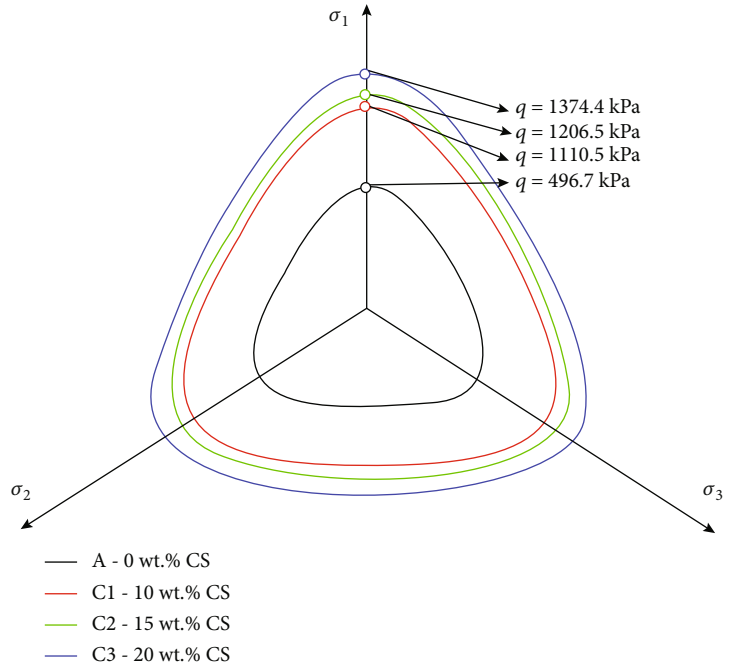


(b)

Figure 13: Continued.

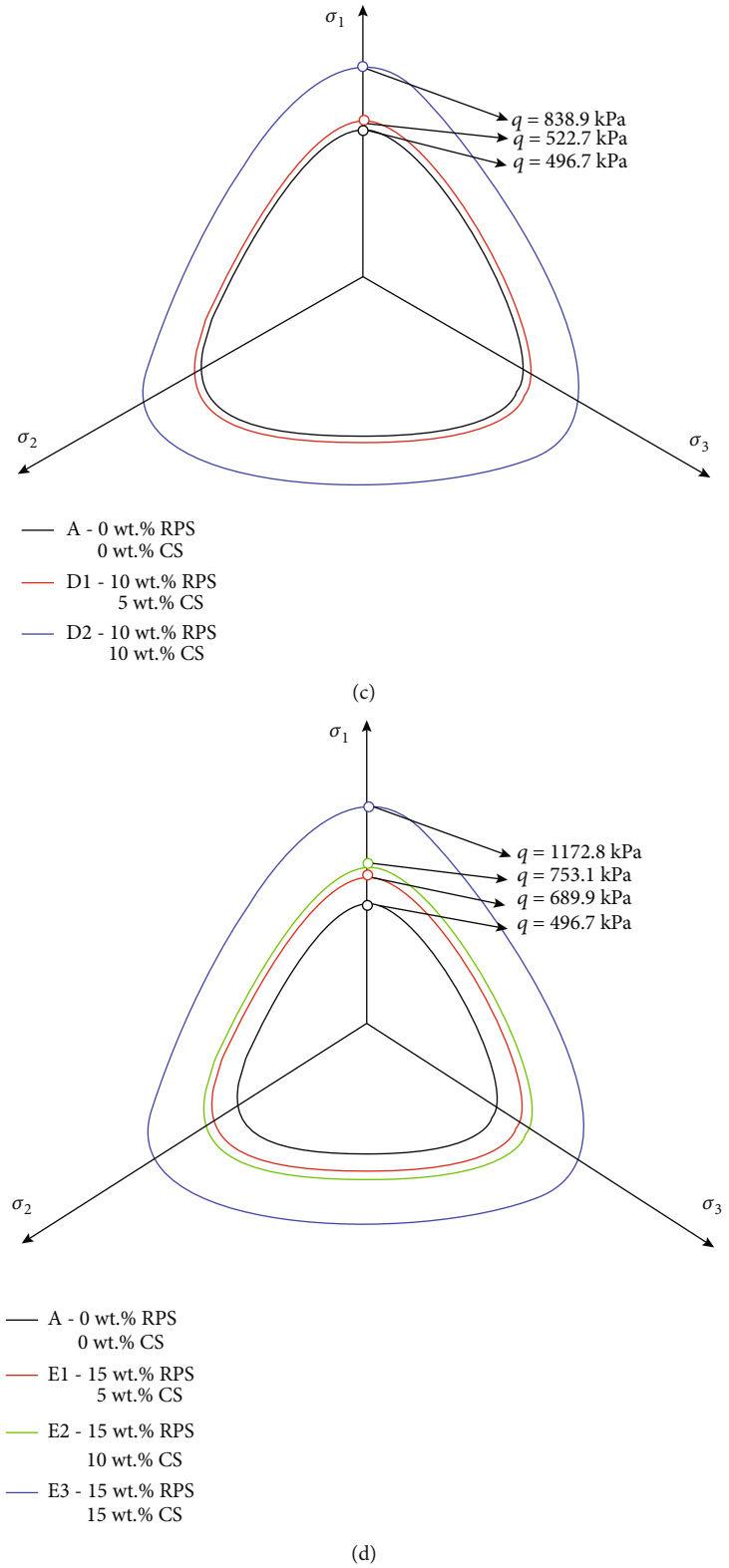


Figure 13: Yield curves of the modified soils under 200 kPa confining pressure: (a) the red Pisha sandstone modified soils; (b) the carbide slag modified soils; and (c, d) the red Pisha sandstone and carbide slag modified soils.

the value of $k_i$ is 1. It can be found that the yield curve shape in the deviatoric plane changes from a complete circle to a curved triangle with the decreasing of $n$.

Figure 11 shows the morphology of yield surfaces under different $n$ values in 3D principal stress space. In order to facilitate observation, $M_0$ is set to different values. And the

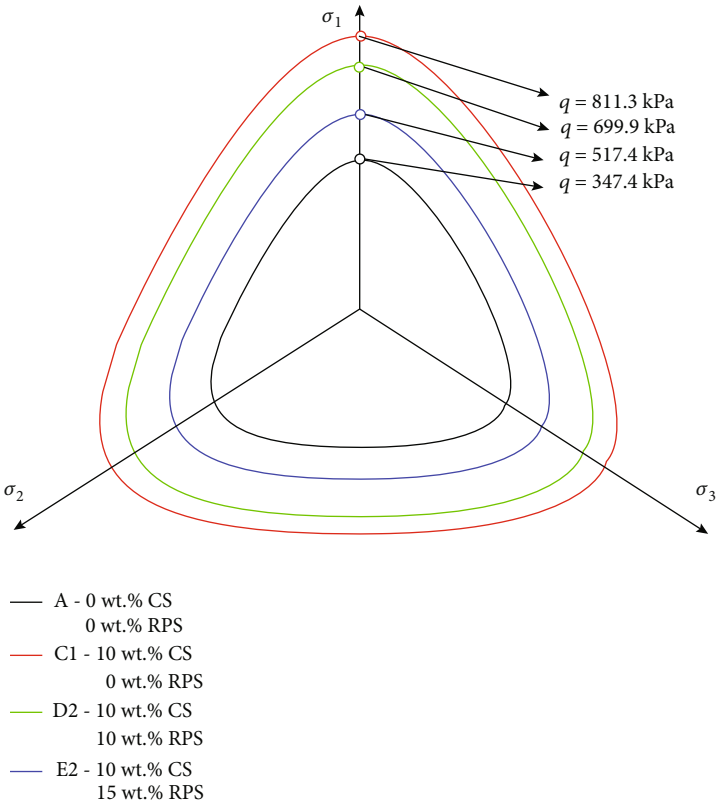


(a)

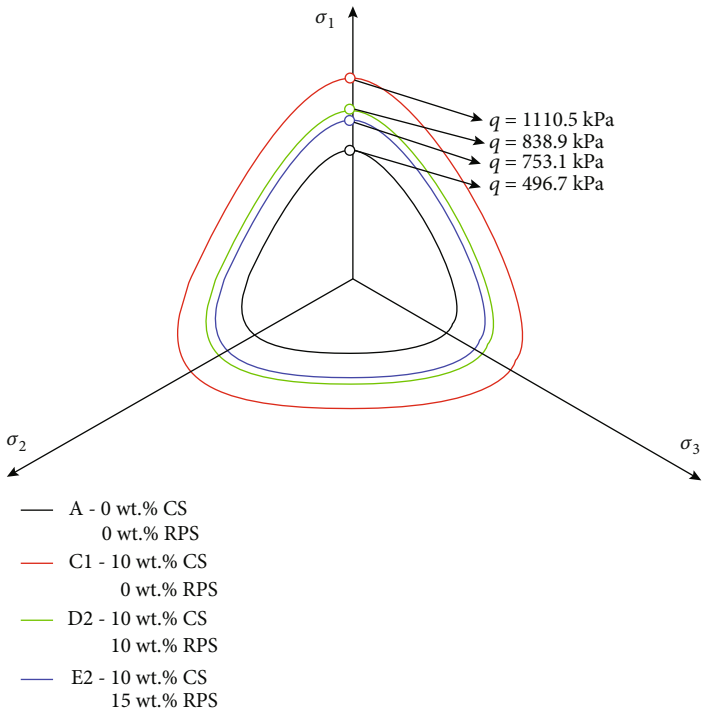


(b)

Figure 14: Continued.

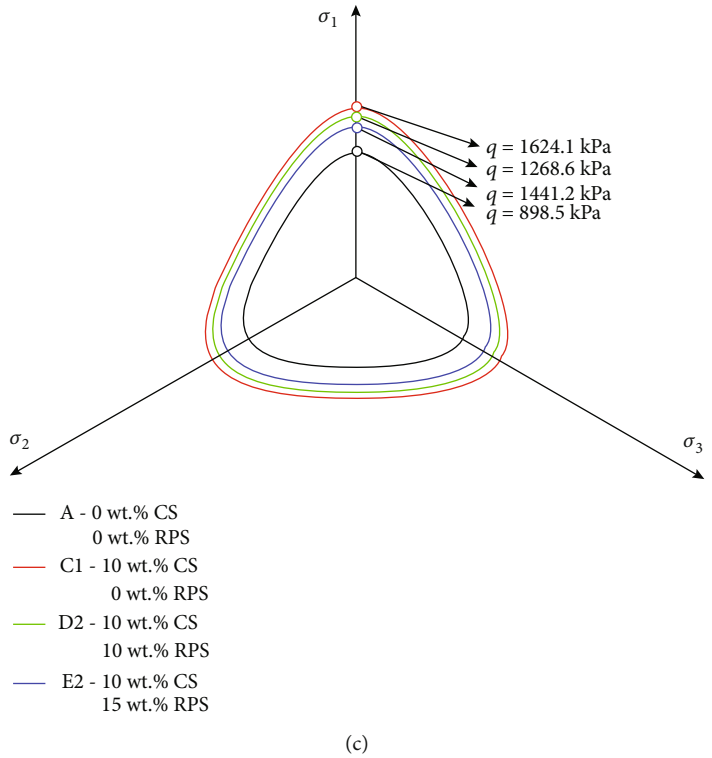


(c)

Figure 14: Yield curves of the 10 wt.% carbide slag modified soils with different red Pisha sandstone contents under different confining pressures: (a) $\sigma_3$ = 100 kPa; (b) $\sigma_3$ = 200 kPa; and (c) $\sigma_3$ = 400 kPa.

space yield surface from inside to outside corresponds to $n$ values of -∞, 0, 1, 2, and 3, respectively. When the value of $n$ changes from small to large, the shapes of the corresponding yield surfaces are gradually transformed from a sharper curved triangle cone to a circular cone. From the above analyses, the generalized criterion has a wide range of application and can describe the yield characteristics of various geotechnical materials well.

In the $p-q-\theta$ space, Equation (17) can be rewritten as

$$\frac{I_1 I_2^{1-n/2}}{I_3^{1-n/3}} = \frac{(3p)\times\left(3p^2-(1/3)q^2\right)^{1-n/2}}{\left(p^3-(1/3)pq^2+(2/27)q^3\cos(3\theta)\right)^{1-n/3}} = k_i. \tag{18}$$

The generalized nonlinear criterion can be expressed as

$$F(p,q,\theta,k_i) = k_i \times \left(p^3-\frac{1}{3}pq^2+\frac{2}{27}q^3\cos(3\theta)\right)^{1-n/3} - (3p)\times\left(3p^2-\frac{1}{3}q^2\right)^{1-n/2} = 0. \tag{19}$$

Obviously, combining with Equations (3) and (19), the above two equations are the modified generalized nonlinear strength and yield criteria expressions for soils. The criterion can scientifically and reasonably describe the nonlinear effects of friction angle, hydrostatic pressure, stress Lode's angle, and admixtures content on strength of geomaterial. Next, the effectiveness of this yield criterion of modified soils will be examined.

*4.2.2. Yield Surface of the Modified Silty Clay.* In the triaxial compression stress state, stress Lode's angle $\theta$ is equal to 0, Equation (19) can be rewritten as [2]

$$F(p,q,\theta,k_i) = k_i \cdot \left(p^3-\frac{1}{3}p\left[M_0(1+p)^{t(m,l)}\right]^2+\frac{2}{27}q^3\right)^{1-n/3} - (3p)\cdot\left(3p^2-\frac{1}{3}\left[M_0(1+p)^{t(m,l)}\right]^2\right)^{1-n/2} = 0. \tag{20}$$

Then, we can determine the yield surface of the modified soil. When $n$ = 1, the yield behavior of the modified soils can be well described by Equation (20). It indicates that the yield surface of the modified soil locates between the SMP criterion ($n$ = 0) and the Lade-Duncan criterion ($n$ = 2). Figure 12 shows the yield curves of pure silty clay under different confining pressures. It can be found that the yield curve gradually expands outward with the increasing of hydrostatic pressure. As the yield curves of the modified soils under different confining pressures are similar, the yield curves of the modified soils under 200 kPa confining pressure are a case study as shown in Figure 13. The yield curves are very close for different admixture contents under a low confining pressure. Thus, a significant change in the shape of the curves cannot be observed. In addition, it can also be found that the yield curve of 15 wt.% red Pisha sandstone

modified soil is located at the innermost, while the shape curve of 10 wt.% red Pisha sandstone modified soil is located at the outermost as shown in Figure 13(a). The curve of sample B3 (20 wt.% red Pisha sandstone) almost coincides with that of pure silty clay (sample A). For carbide slag modified soils, the shape curve gradually expands outward with the increasing of carbide slag content as shown in Figure 13(b). For red Pisha sandstone and carbide slag modified soils when the content of red Pisha sandstone is constant, the shape curve gradually expands outward with the increasing of carbide slag content as shown in Figures 13(c) and 13(d). It can be found that the yield stress of the modified soil increases with the increase of carbide slag content.

The yield curves of the modified soils with different red Pisha sandstone contents under different confining pressures when carbide slag content is 10 wt.% are shown in Figure 14. The innermost curve is the yield curve of pure silty clay. The curve gradually shrinks inward with the increase of the red Pisha sandstone content. The yield stress reaches a minimum value when the red Pisha sandstone content is equal to 15 wt.%, while it reaches a maximum value when the red Pisha sandstone content is 0 wt.%. It shows that the yield stress of the modified soils decreases gradually with the increase of the red Pisha sandstone content when the carbide slag content is a constant.

## 5. Conclusions

A series of triaxial compression tests have been carried out for modified silty clay with red Pisha sandstone and carbide slag in this study, and the strength and yield behaviors of the modified silty clay have been studied. The following conclusions can be made:

(1) The strength reaches a minimum value when the red Pisha sandstone content equals to 15 wt.% and the carbide slag content equals to 0 wt.%, while it reaches a maximum value when the red Pisha sandstone and the carbide slag contents equal to 0 wt.% and 20 wt.%, respectively. The influence of the red Pisha sandstone on strength nonlinear degree is greater than that of the carbide slag

(2) The strength variation of the modified soils is obviously nonlinear with the hydrostatic pressure and admixtures content increasing, and the nonlinear strength can be described by a modified critical state function

(3) The yield behavior of the modified soil can be described by a generalized nonlinear criterion, and the yield surface of the modified soil is located between the SMP criterion and the Lade-Duncan criterion

## Data Availability

The data is included in the manuscript.

## Conflicts of Interest

The authors declare that they have no conflicts of interest.

## Acknowledgments

This research was supported by the Key Research Program of the Chinese Academy of Sciences (Grant No. ZDRW-ZS-2020-1), the Key Research Program of Frontier Sciences of Chinese Academy of Sciences (Grant No. QYZDY-SSW-DQC015), and the Project of the State Key Laboratory of Frozen Soil Engineering (Grant No. SKLFSE-ZQ-57).

## References

[1] Y. P. Zhang, *Research on Dynamic Properties and Deformation Characteristics of Subgrade Filling Modified by Oil Shale Wastes in Seasonally Frozen Area*, Jilin University, 2019.

[2] Z. W. Zhou, W. Ma, S. J. Zhang, H. du, Y. Mu, and G. Li, "Multiaxial creep of frozen loess," *Mechanics of Materials*, vol. 95, pp. 172–191, 2016.

[3] Z. L. Chen, *The Study of Strength Criterion and Constitutive Model for Structured Soil*, Harbin Institute of Technology, 2016.

[4] Z. W. Zhou, W. Ma, S. J. Zhang, Y. Mu, and G. Li, "Experimental investigation of the path-dependent strength and deformation behaviours of frozen loess," *Engineering Geology*, vol. 265, p. 105449, 2020.

[5] Z. W. Zhou, G. Y. Li, M. D. Shen, and Q. Wang, "Dynamic responses of frozen subgrade soil exposed to freeze-thaw cycles," *Soil Dynamics and Earthquake Engineering*, vol. 152, p. 107010, 2022.

[6] Z. Y. Yin, P. Y. Hicher, and Y. F. Jin, *Practice of Constitutive Modelling for Saturated Soils*, Springer, Singapore, 2020.

[7] Y. P. Yao, D. C. Lu, A. Zhou, and B. Zou, "Generalized nonlinear strength theory and transformed stress space," *Science in China(Series E:Technological Sciences)*, vol. 47, no. 6, pp. 691–709, 2004.

[8] G. Mortara, "A new yield and failure criterion for geomaterials," *Geotechnique*, vol. 58, no. 2, pp. 125–132, 2008.

[9] M. D. Liu and B. N. Indraratna, "General strength criterion for geomaterials including anisotropic effect," *International Journal of Geomechanics*, vol. 11, no. 3, pp. 251–262, 2011.

[10] Y. M. Lai, M. K. Liao, and K. Hu, "A constitutive model of frozen saline sandy soil based on energy dissipation theory," *International Journal of Plasticity*, vol. 78, pp. 84–113, 2016.

[11] M. K. Liao, Y. M. Lai, and C. Wang, "A strength criterion for frozen sodium sulfate saline soil," *Canadian Geotechnical Journal*, vol. 53, no. 7, pp. 1176–1185, 2016.

[12] Y. H. Zhao, Y. M. Lai, W. S. Pei, and F. Yu, "An anisotropic bounding surface elastoplastic constitutive model for frozen sulfate saline silty clay under cyclic loading," *International Journal of Plasticity*, vol. 129, pp. 0749–6419, 2020.

[13] M. D. Shen, Z. W. Zhou, and S. J. Zhang, "Effect of stress path on mechanical behaviors of frozen subgrade soil," *Road Materials and Pavement Design*, vol. 23, no. 5, pp. 1061–1090, 2021.

[14] Z. B. Dong and P. Wang, "Study on stability of high fill embankment with silty clay modified by lime and fly ash," *Fly Ash Comprehensive Utilization*, vol. 1, pp. 53–56, 2019.

[15] Y. L. Yi, L. Y. Gu, S. Y. Liu, and A. J. Puppala, "Carbide slag-activated ground granulated blastfurnace slag for soft clay

stabilization," *Canadian Geotechnical Journal*, vol. 52, no. 5, pp. 656–663, 2015.

[16] L. F. Wang, X. X. Xie, and T. Wang, "Study on mechanical properties and constitutive model of remolding lime soil," *Bulletin of Science and Technology*, vol. 35, no. 11, pp. 195–200, 2019.

[17] X. C. Ren, *Experimental Study of Nano-Silica on the Mechanical Properties of Frozen (Thawing)-Soil*, Lanzhou University, 2016.

[18] H. B. Wang, *Study about Road Performance and Bearing Capacity Mechanism of Fly Ash*, Hunan University, 2014.

[19] Y. H. Liu, D. Q. Li, and F. Ming, "Modification of silty clay subgrade filler with red Pisha sandstone and carbide slag in seasonally frozen regions," *Environmental Earth Sciences*, vol. 81, no. 9, p. 272, 2022.

[20] GBT 50123, *China Geotechnical Test Standards*, Ministry of Housing and Urban-Rural Development of the People's Republic of China, 2019.

[21] C. M. Li, J. L. Dong, S. B. Zhao, H. Liu, W. Yao, and L. Wang, "Development of low cost supplementary cementitious materials utilizing thermally activated Pisha sandstone," *Construction and Building Materials*, vol. 174, pp. 484–495, 2018.

[22] J. L. Dong, C. M. Li, H. Liu, L. Zhang, and J. Liu, "Investigating the mechanical property and reaction mechanism of geopolymers cement with red Pisha sandstone," *Construction and Building Materials*, vol. 201, pp. 641–650, 2019.

[23] Q. Zhang, Z. Song, X. Li, J. Wang, and L. Liu, "Deformation behaviors and meso-structure characteristics variation of the weathered soil of Pisha sandstone caused by freezing-thawing effect," *Cold Regions Science and Technology*, vol. 167, pp. 102864.1–102864. 17, 2019.

[24] Y. J. Wu, J. P. Li, H. B. Jiang, and G. Q. Kong, "Consolidation and permeability characteristics of transparent clay with different grain composition," *Journal of Northeastern University (Natural Science)*, vol. 41, no. 6, pp. 117–122, 2020.

[25] Q. S. Chen, Y. X. Li, H. L. Xiao, W. Peng, and J. W. Wang, "Shear behavior of calcareous sands improved by polyurethane foam adhesive considering effects of particle size distribution," *Science Technology and Engineering*, vol. 20, no. 28, pp. 11718–11724, 2020.

[26] C. M. Li, T. Zhang, and L. Wang, "Effect of dosage of fly ash and NaOH on properties of Pisha sandstone-based mortar," *ACI Materials Journal*, vol. 113, no. 2, pp. 173–183, 2016.

[27] M. Y. Li, X. L. Li, S. H. Chen, Q. Zhang, P. Chang, and S. Y. Wu, "Experiment study on strength and stress-strain curve characteristic of Pisha-sandstone remolded soil," *Journal of Drainage and Irrigation Machinery Engineering*, vol. 36, no. 2, pp. 179–184, 2018.

[28] Z. S. Liang, C. Q. Yang, and Z. R. Wu, "Study on mechanical properties of Pisha sandstone solidified body with W-OH composite," *Yellow River*, vol. 38, no. 6, pp. 30–34, 2016.

[29] N. J. Jiang, Y. J. Du, S. Liu, M. L. Wei, S. Horpibulsuk, and A. Arulrajah, "Multi-scale laboratory evaluation of the physical, mechanical, and microstructural properties of soft highway subgrade soil stabilized with calcium carbide residue," *Canadian Geotechnical Journal*, vol. 53, pp. 373–383, 2016.

[30] X. B. Wang, X. Yan, and X. Y. Li, "Environmental safety risk for application of industrial solid wastes carbide slag in soil," *Soil and Fertilizer Sciences in China*, vol. 1, no. 4, pp. 1–8+95, 2019.

[31] A. Kampala, S. Horpibulsuk, A. Chinkullijniwat, and S. L. Shen, "Engineering properties of recycled calcium carbide residue stabilized clay as fill and pavement materials," *Construction & Building Materials*, vol. 46, no. 9, pp. 203–210, 2013.

[32] K. H. Roscoe and J. B. Burland, "On the generalised stress-strain behaviour of 'wet' clay," in *Engineering Plasticity*, pp. 535–609, Cambridge University Press, 1968.

[33] Y. H. Zhao, Y. M. Lai, J. Zhang, and C. Wang, "A nonlinear strength criterion for frozen sulfate saline silty clay with different salt contents," *Advances in Materials Science and Engineering*, 2018.